Assessing the photochemical transformation pathways of acetaminophen relevant to surface waters: transformation kinetics, intermediates, and modeling

(Article begins on next page)

05 November 2024

ASSESSING THE PHOTOCHEMICAL TRANSFORMATION PATHWAYS OF ACETAMINOPHEN RELEVANT TO SURFACE WATERS: TRANSFORMATION KINETICS, INTERMEDIATES, AND MODELLING

Elisa De Laurentiis,[a] Carsten Prasse,[b] Thomas A. Ternes,[b] Marco Minella,[a] Valter Maurino,[a] Claudio Minero,[a] Mohamed Sarakha,[c,d] Marcello Brigante,[c,d] and Davide Vione [a,e]∗

[a] *Università degli Studi di Torino, Dipartimento di Chimica, Via P. Giuria 5, 10125 Torino, Italy.*
   http://www.chimicadellambiente.unito.it

[b] *Federal Institute of Hydrology (BfG), Referat G2, Am Mainzer Tor 1, 56068 Koblenz, Germany.*

[c] *Clermont Université, Université Blaise Pascal, Institut de Chimie de Clermont-Ferrand, BP 10448, F-63000 Clermont-Ferrand, France.*

[d] *CNRS, UMR 6296, ICCF, BP 80026, F-63177 Aubière, France.*

[e] *Università degli Studi di Torino, Centro Interdipartimentale NatRisk, Via L. Da Vinci 44, 10095 Grugliasco (TO), Italy. http://www.natrisk.org*

∗ Corresponding author. Tel. +39-011-6705296. E-mail: *davide.vione@unito.it*

Abstract

This work shows that the main photochemical pathways of acetaminophen (APAP) transformation in surface waters would be direct photolysis (with quantum yield of $(4.57\pm0.17)\cdot10^{-2}$), reaction with $CO_3^{-\bullet}$ (most significant at pH > 7, with second-order rate constant of $(3.8\pm1.1)\cdot10^8 \ M^{-1} \ s^{-1}$) and possibly, for dissolved organic carbon higher than 5 mg C L^{-1}, reaction with the triplet states of chromophoric dissolved organic matter ($^3CDOM^*$). The modelled photochemical half-life time of APAP in environmental waters would range from days to few weeks in summertime, which suggests that the importance of phototransformation might be comparable to biodegradation. APAP transformation by the main photochemical pathways yields hydroxylated derivatives, ring-opening compounds as well as dimers and trimers (at elevated concentration levels). In the case of $^3CDOM^*$ (for which the triplet state of anthraquinone-2-sulphonate was used as proxy), ring rearrangement is also hypothesised. Photochemistry would produce different transformation products (TPs) of APAP than microbial biodegradation or human metabolism, thus the relevant TPs might be used as markers of APAP photochemical reaction pathways in environmental waters.

Keywords: acetaminophen; paracetamol; acetyl-*para*-aminophenol; direct and sensitised photolysis; pharmaceuticals and personal care products (PPCPs); surface-water photochemistry.

1. Introduction

The anti-inflammatory and antipyretic drug acetaminophen (N-(4-hydroxyphenyl)ethanamide) is one of the most widely sold over-the-counter drugs worldwide (Newson et al., 2000; McBride, 2011), and it ranks #1 in the list of pharmaceuticals marketed in many European countries (EFPIA, 2006). Its worldwide use is perhaps best exemplified by the multitude of names it has been given, among which are paracetamol, acetaminophen and acetyl-*para*-aminophenol, from which its most common acronym (APAP) has been derived. In this paper as well, APAP will be used for acetaminophen.

Like other popular pharmaceuticals, APAP and its metabolites are released into wastewater by excretion and probably because of incorrect disposal *via* the toilet, which causes a relevant load at the inlet of wastewater treatment plants (WWTPs) (Del Rio et al., 2013). APAP is rather effectively degraded by biological processes, but appreciable concentrations can still be found at WWTP outlets or in surface waters (Stamatis and Konstantinou, 2013). The large use of APAP ensures that quite elevated loads reach the natural environment despite degradation in WWTPs (Morasch et al., 2010; Chiron et al., 2010; Gros et al., 2010). For this reason, it is very important to investigate the fate of APAP in surface waters, where it is potentially toxic to *e.g.* aquatic invertebrates (Jones et al., 2002).

APAP biodegradation would take place in a time scale from days to months (Hari et al., 2005; Jones et al., 2005; Yamamoto et al., 2005), and sequestration contributes to its removal from water in contact with sediment (Loeffler et al., 2005). Recent research has highlighted that APAP is also transformed by photochemical processes that can be competitive with biodegradation (Yamamoto et al., 2009; Peuravuori, 2012). Photochemical reactions are an important class of abiotic pathways for dissolved pollutants in surface waters (Tixier et al., 2003). They are usually divided into direct photolysis, where absorption of sunlight by the pollutant causes its transformation, and indirect photodegradation. In the latter case, photoactive compounds called photosensitisers (such as nitrate, nitrite and chromophoric dissolved organic matter, CDOM) absorb sunlight and produce reactive species such as $^\bullet OH$, $CO_3^{-\bullet}$, $^1O_2$ and CDOM triplet states, $^3CDOM^*$ (Gerecke et al., 2001; Boreen et al., 2003; Canonica et al., 2005; Page et al., 2011). In the case of APAP, photodegradation has been investigated in the presence of nitrate and CDOM although the role of the possible photoreactive transients (*e.g.* $^\bullet OH$, $^1O_2$ and $^3CDOM^*$) was not differentiated (Peuravuori, 2012). However, as it will be demonstrated in the present paper, one of the most important pathways of APAP phototransformation (reaction with $CO_3^{-\bullet}$) has not been taken into account so far. Therefore, the importance of photochemistry in the environmental fate of APAP might have been underestimated.

This work studies the kinetics of APAP phototransformation pathways of potential environmental significance, by determining the direct photolysis quantum yield and the reaction rate constants with $^\bullet OH$, $CO_3^{-\bullet}$, $^1O_2$ and $^3CDOM^*$. These data allow the modelling of APAP lifetime, as a function of environmental conditions such as water chemistry and depth. The study of

transformation intermediates (also called transformation products, TPs) can be very important in the environmental (photo)chemistry of xenobiotics, because sometimes TPs are of higher concern than the parent molecule. Examples are the cases of triclosan (Kliegman et al., 2013) and carbamazepine (Donner et al., 2013). Therefore, the TPs of APAP formed *via* the main photochemical reaction pathways were identified to get insight into the environmental conditions that would favour their photoassisted occurrence.

2. Experimental section

2.1. Reagents and materials

Acetaminophen (APAP, purity grade 98%), anthraquinone-2-sulphonic acid, sodium salt (AQ2S, 97%), hydroquinone (HQ, 98%), 1-nitronaphthalene (1NN, 99%), furfuryl alcohol (98%), $NaNO_3$ (>99%), $NaHCO_3$ (98%), $Na_2HPO_4 \cdot 2\ H_2O$ (98%), $NaH_2PO_4 \cdot H_2O$ (98%), $HClO_4$ (70%) and H_3PO_4 (85%) were purchased from Aldrich, NaOH (99%), H_2O_2 (35%) and 2-propanol (LiChrosolv gradient grade) from VWR Int., methanol (gradient grade) from Carlo Erba, Rose Bengal (RB) from Alfa Aesar.

2.2. Irradiation experiments

The kinetic parameters relevant to the main photochemical processes that would involve APAP in surface waters (direct photolysis and reaction with $^\bullet OH$, $CO_3^{-\bullet}$, $^1O_2$ and $^3CDOM^*$) were determined by laboratory measurements. These results allow for the modelling of the lifetime of pollutants as a function of environmental variables (Vione et al., 2011; De Laurentiis et al., 2012a). AQ2S was used as CDOM proxy to assess reactivity between APAP and $^3CDOM^*$. Reasons for this choice are the widespread occurrence of quinones in CDOM (Cory and McKnight, 2005) and the fact that irradiation of AQ2S, unlike other triplet sensitisers, does not yield interfering transients such as $^\bullet OH$ or $^1O_2$. The triplet state $^3AQ2S^*$ is not quenched by oxygen because it quickly reacts with H_2O to form two water adducts, which evolve into hydroxyderivatives without producing $^\bullet OH$ (Maddigapu et al., 2010). AQ2S initial concentration was 0.1 mM, to limit the additional complication represented by reaction between the excited and ground states of AQ2S (Bedini et al., 2012).

Solutions (5 mL) were irradiated in Pyrex glass cells (4.0 cm diameter, 2.3 cm height, 295 nm cut-off wavelength) and magnetically stirred during irradiation. Irradiation of APAP alone to study direct photolysis, of APAP + nitrate or APAP + H_2O_2 to study reaction with $^\bullet OH$, and of APAP + nitrate + bicarbonate to study reaction with $CO_3^{-\bullet}$ was carried out under a 20 W Philips TL 01 UVB lamp, with emission maximum at 313 nm. The lamp had 3.0±0.2 W m^{-2} UV irradiance in the 300-400 nm range, measured with a power meter by CO.FO.ME.GRA. (Milan, Italy) equipped with a UV-sensitive probe. The incident photon flux in solution was actinometrically determined using the ferrioxalate method (Kuhn et al., 2004). By knowing, as a function of wavelength, the fraction of radiation absorbed by $Fe(C_2O_4)_3^{3-}$, the quantum yield of Fe^{2+} photoproduction and the shape of the

3

lamp spectrum, it is possible to use the measured formation rate of Fe^{2+} to determine the value of the incident spectral photon flux density $p°(\lambda)$. The photon flux of the TL 01 lamp between 300 and 500 nm was $P_o = \int_\lambda p°(\lambda)d\lambda = (2.0\pm0.1)\cdot10^{-5}$ Einstein L^{-1} s^{-1}. APAP transformation photosensitised by AQ2S was studied under a 40 W Philips TLK 05 UVA lamp, with emission maximum at 365 nm, 28 ± 2 W m^{-2} UV irradiance (300-400 nm), and $(2.1\pm0.2)\cdot10^{-5}$ Einstein L^{-1} s^{-1} incident photon flux in solution. The photodegradation of APAP sensitised by Rose Bengal (RB) *via* $^1O_2$ was studied under a Philips TL D 18W/16 yellow lamp, with emission maximum at 545 nm and 11 ± 1 W m^{-2} irradiance in the visible, measured with the CO.FO.ME.GRA. power meter equipped with a probe sensitive to visible radiation.

The choice of the lamps had the purpose of exciting each photosensitiser as selectively as possible, to minimise unwanted processes. Once reaction rate constants and photolysis quantum yields were experimentally obtained, the effect of actual sunlight could be assessed by means of a model approach (*vide infra*). The direct photolysis of APAP was studied under UVB upon consideration of its absorption spectrum, measured with a Varian Cary 100 Scan UV-Vis spectrophotometer. The same instrument was used to measure the absorption spectra of nitrate, AQ2S and RB. The various emission and absorption spectra are reported in Figure 1. Unless otherwise reported, the initial concentration of APAP in the irradiation experiments was 20 µM and the solution pH was around 7. The APAP concentration was chosen to enable easy quantification by HPLC, without the need of using pre-concentration steps that would introduce substantial variability in the data. Considering that irradiation experiments were aimed at deriving kinetic parameters for model simulations (see section 2.7) and not to directly simulate environmental conditions, the use of a relatively high APAP concentration would not introduce a significant bias in the results. Furthermore, the chosen concentration should not affect APAP direct photolysis (Bedini et al., 2012), which followed a pseudo-first order trend. The limits of detection and quantification for APAP by HPLC-DAD were around 0.1 and 0.3 µM, respectively.

2.3. Monitoring of APAP transformation

The irradiated solutions were analysed by high-performance liquid chromatography (HPLC-DAD) on a VWR-Hitachi LaChrom Elite instrument, equipped with autosampler L-2200 (60 µL sample volume), quaternary pump L-2130 for low-pressure gradients, a reverse-phase column Merck LiChrocart RP-C18 packed with LiChrospher 100 RP-18 (125 mm × 4.6 mm × 5 µm), diode array detector (DAD) L-2455, and control software EZChrome Elite. For the monitoring of APAP and HQ, elution was carried out with 5% methanol (A) and 95% aqueous H_3PO_4 at pH 2.8 (B), with a total flow rate of 1.0 mL min^{-1}. Retention times were 3.5 min for hydroquinone (HQ) and 8.8 min for APAP, column dead time being 0.9 min. Tyrosine and APAP were eluted with the following gradient: 2% A for 5 min, up to 80% A in 1 min and kept for 6 min, then down to 2% A in 1 min and kept for 10 min (post-run equilibration), always at 1.0 mL min^{-1} flow rate. Retention times were 8.3 min for APAP and 2.4 min for tyrosine. APAP was monitored at 245 nm, tyrosine at 274

nm and HQ at 220 nm. The time evolution of furfuryl alcohol to quantify the formation rate of $^1O_2$ under the yellow lamp was also monitored by HPLC-DAD, as reported in Minella et al. (2011).

2.4. Identification of APAP TPs

For TPs elucidation, the same irradiation conditions were used as described above. Samples were taken at different time intervals (initial concentration of APAP: 1 mmol L^{-1}) and analysed via high-resolution mass spectrometry using a TripleTOF instrument (TripleTOF 5600; AB Sciex, Darmstadt, Germany) connected to an 1260 HPLC system (Agilent, Waldbronn, Germany) with an electrospray ionisation (ESI) interface (LC-ESI-QTOF/MS/MS). The ion source parameters were: temperature (TEM) 550°C; ion spray floating voltage (ISVF) 4500 V; curtain gas (CUR) 25 L min^{-1}; ion source gases (GS1 and GS2) 30 psi and 40 psi, respectively. Chromatographic separation was carried out on a 4 μm Synergi Hydro-RP column (150 × 3 mm i.d.) equipped with a SecurityGuard column (4 × 3 mm i.d.; Phenomenex, Aschaffenburg, Germany). Flow rate was set to 400 μL min^{-1} using 0.1 % formic acid (A) and methanol + 0.1 % formic acid (B) as mobile phases. The percentage of (A) was changed linearly as follows: 0-10 min, 100%; 25 min, 10%; 28 min, 10%; 29 min, 100%; 35 min, 100%. Full scans were performed in both positive and negative ESI-mode with a mass range of 50 to 650 m/z. The resolution was set at 40,000 (FWHM at 400 m/z). For the acquisition of MS/MS data, information-dependent acquisition (IDA) was used with a threshold of 100 cps and a mass tolerance of 50 mDa. The declustering potential (DP) and collision energy (CE) were set to 50 V and 10 eV, respectively. An accumulation time of 250 ms was used for TOF-MS survey scans and dependent MS/MS scans. The instrument was calibrated automatically every five samples using an injector system (CDS, Calibrant Delivery System), obtaining an accuracy of < 1 ppm. Acquired full scan and MS/MS data were mined using PeakView and MarkerView software (both by AB Sciex).

2.5. Laser flash photolysis measurements

The carbonate radical was produced *via* an electron transfer reaction from CO_3^{2-} to the excited triplet state of 1-nitronaphthalene (^{3}1NN), which was generated by laser flash excitation (Brigante et al., 2010). It was used the third harmonic (λ_{exc} = 355 nm) of a Quanta Ray GCR 130-01 Nd:YAG laser system instrument, placed in a right-angle geometry with respect to the monitoring light beam. The single pulses were *ca.* 9 ns in duration, with an energy of ~90 mJ/pulse. To avoid photodegradation of the solution due to multiple laser shots, a flow cell was used that was connected to a peristaltic pump, allowing fresh solution to continuously purge the laser-exposed volume.

The produced transient species were monitored by means of time-resolved absorption spectroscopy, using a pulsed xenon lamp (150 W), monochromator and a photomultiplier (1P28). A spectrometer control unit was used for synchronising the pulsed light source and programmable shutters with the laser output. The signal from the photomultiplier was digitised by a programmable

digital oscilloscope (HP54522A). A 32 bits RISC processor kinetic spectrometer workstation was used to analyse the digitised signal. Experiments were performed at room temperature (~ 293 K).

In the presence of 0.1 M CO_3^{2-}, the pseudo-first order decay constant of ^{3}1NN monitored at 620 nm increased from ~ $6.3 \cdot 10^5$ s^{-1} (mostly due to quenching by oxygen; Brigante et al., 2010) to $2.3 \cdot 10^6$ s^{-1}. A long-lived transient appeared, which was identified as $CO_3^{-\bullet}$ on the basis of its absorption maximum around 600 nm (Weeks and Rabani, 1966). The time evolution of the absorption at 600 nm was fitted with a double exponential decay equation, to take into account the presence of both ^{3}1NN and $CO_3^{-\bullet}$.

2.6. Kinetic data treatment

The time trend of APAP under irradiation followed pseudo-first order kinetics. Reaction rates were determined by fitting time evolution data with equations of the form $C_t \, C_o^{-1} = exp(-k\,t)$, where C_t is the concentration of APAP at the irradiation time t, C_o its initial concentration, and k the pseudo-first order degradation rate constant. The initial degradation rate is $R_{APAP} = k \, C_o$. The time evolution of HQ is the result of two consecutive and independent pseudo-first order processes, namely formation from APAP and photodegradation. Kinetic modelling yields $HQ_t = k_{HQ}' C_o \, (k_{HQ}'' - k_{APAP})^{-1} \, (e^{-k_{APAP} t} - e^{-k_{HQ}'' t})$, where C_o and k_{APAP} are as above, HQ_t is the concentration of HQ at the time t, k_{HQ}' the pseudo-first order rate constant of HQ formation from APAP, and k_{HQ}'' the pseudo-first order rate constant of HQ transformation. The initial formation rate of HQ is $R_{HQ}' = k_{HQ}' \, C_o$. The reported errors on the rates ($\pm\sigma$) were derived by curve fitting and depended on the scattering of experimental data around the fit curve. The reproducibility of repeated runs was about 15-20%.

2.7. Photochemical modelling

A detailed description of the model that we have used in this work is reported in several previous publications (see for instance Minella et al., 2013 or Ruggeri et al., 2013). Moreover, a software application has been recently developed (APEX: Aqueous Photochemistry of Environmentally-occurring Xenobiotics). It is freely available (including the User's Guide that contains a comprehensive account of model equations) at *http://chimica.campusnet.unito.it/do/didattica.pl/Quest?corso=7a3d*. The model has been validated by comparison with field data of phototransformation of pharmaceutical compounds (Vione et al., 2011; De Laurentiis et al., 2012a).

APEX predicts steady-state concentrations of $^\bullet OH$, $CO_3^{-\bullet}$, $^1O_2$ and $^3CDOM*$ based on water chemistry and depth and on the spectral photon flux density of sunlight. The model also predicts pollutant reaction kinetics (pseudo-first order rate constants) due to $^\bullet OH$, $CO_3^{-\bullet}$, $^1O_2$ and $^3CDOM*$, as well as kinetics of direct photolysis. Required input data are pollutant absorption spectrum, photolysis quantum yield and second-order rate constants with $^\bullet OH$, $CO_3^{-\bullet}$, $^1O_2$ and $^3CDOM*$. Formation yields of TPs *via* the different photochemical pathways are required to model their formation rate constants. The standardised time unit in the model is a summer sunny day (SSD),

equivalent to fair-weather 15 July at 45°N latitude (Vione et al., 2011). By so doing, it is possible to take into account the day-night cycle and to use a time unit of definite duration that relates to outdoor conditions.

An additional issue is that sunlight is not vertically incident over the water surface. The solar zenith angle should be considered, although refraction deviates the light path in water towards the vertical. Because of this phenomenon, the path length l of light in water is longer than the water depth d: on 15 July at 45°N it is $l = 1.05\ d$ at noon, and $l = 1.17\ d$ at ±3 h from noon that is a reasonable daily average.

3. Results and Discussion

3.1. APAP phototransformation kinetics

The kinetics of APAP transformation were determined upon direct photolysis and reaction with $^\bullet OH$, $CO_3^{-\bullet}$, $^1O_2$ and $^3CDOM^*$ (with AQ2S as CDOM proxy as already explained). The same experimental protocol has been used for other compounds (see for instance Maddigapu et al., 2011; Vione et al., 2011; De Laurentiis et al., 2012a). Details and results of the relevant experiments are reported as Supplementary Material (hereafter SM). Table 1 summarises the data of photolysis quantum yields and reaction rate constants for APAP. The reaction rate constant between APAP and $^3AQ2S^*$ is quite high, although it is comparable to those reported for ibuprofen and 4-isobutylacetophenone with $^3AQ2S^*$ (Ruggeri et al., 2013). It is also about 3-4 times higher than the rate constants of the triplet state of benzophenone (a CDOM proxy as well) with a range of phenylurea herbicides (Canonica et al., 2006), which might be less reactive than phenolic APAP toward triplet sensitisers. However, the fact that the rate constant of APAP with $^3AQ2S^*$ is higher than that with $^\bullet OH$ might suggest a peculiar reactivity between $^3AQ2S^*$ and APAP. Therefore, the possibility will be taken into account that $k_{^3CDOM^*,APAP} < k_{^3AQ2S^*,APAP}$. As far as reactivity with $CO_3^{-\bullet}$ is concerned, SM reports the results of a semi-quantitative screening study that used nitrate and bicarbonate under irradiation (Vione et al., 2009a). The outcome is that the reaction between APAP and $CO_3^{-\bullet}$ has potential environmental significance, thus the reaction rate constant was determined by making use of laser flash photolysis and steady irradiation.

In the case of laser irradiation, proper detection of $CO_3^{-\bullet}$ required very basic conditions (see SM), where APAP would be dissociated ($pK_a = 9.5$; Jones et al., 2002). Therefore, the reaction rate constant between $CO_3^{-\bullet}$ and undissociated APAP (which would prevail in surface waters) was measured by means of competition kinetics with tyrosine under steady irradiation. Figure 2 reports the time trends of APAP and tyrosine (10 µM initial concentration for both compounds) upon UVB irradiation of 0.01 M $NaNO_3$ + 0.10 M $NaHCO_3$ (pH 8.2). The degradation of APAP was significantly faster than that of tyrosine, with experimental pseudo-first order rate constants $k_{APAP} = 1.90\pm0.20$ h^{-1} and $k_{Tyr} = 0.265\pm0.039$ h^{-1}, respectively. The ratio of the rate constants is $\Re = k_{APAP}$

$k_{\text{Tyr}}^{-1} = 7.17 \pm 1.81$. The direct photolysis of the two substrates could be neglected under the adopted experimental conditions.

The UVB photolysis of nitrate produces $^{\bullet}OH$ radicals, which can react with carbonate and bicarbonate to yield $CO_3^{-\bullet}$ (with second-order rate constants of $3.9 \cdot 10^8$ and $8.5 \cdot 10^6$ M^{-1} s^{-1}, respectively; Buxton et al., 1988), as well as with APAP and tyrosine. The reaction rate constant between tyrosine and $^{\bullet}OH$ radicals ($1.3 \cdot 10^{10}$ M^{-1} s^{-1}; Buxton et al., 1988) is almost one order of magnitude higher than for APAP and $^{\bullet}OH$ (see Table 1). Although the rate constant between APAP and $^{\bullet}OH$ was determined at pH 7 (see SM), no significant modification is expected at pH 8.2 because the protonated form of APAP would prevail in both cases. Therefore, the most important competition for $^{\bullet}OH$ radicals would take place between tyrosine and CO_3^{2-}/HCO_3^-. Based on the reported second-order reaction rate constants (Buxton et al., 1988) and on the concentration values of the relevant compounds, one gets that 98% of photogenerated $^{\bullet}OH$ radicals would oxidise CO_3^{2-}/HCO_3^- to give $CO_3^{-\bullet}$, which would then react with either tyrosine or APAP. A scheme summarising the reaction pathways involved and their branching ratios is reported as SM (Figure S6).

Considering the competition kinetics of dissolved species for $^{\bullet}OH$ and $CO_3^{-\bullet}$ and assuming $R_{\bullet_{OH}}$ as the formation rate of $^{\bullet}OH$ radicals, one has that: *(i)* the reaction rate of $^{\bullet}OH$ radicals with tyrosine is $R_{\bullet_{OH}}^{Tyr} = 1.8 \cdot 10^{-2}$ $R_{\bullet_{OH}}$; *(ii)* the reaction rate of $^{\bullet}OH$ with APAP is $R_{\bullet_{OH}}^{APAP} = 2 \cdot 10^{-3}$ $R_{\bullet_{OH}}$; *(iii)* the reaction rate of $^{\bullet}OH$ with CO_3^{2-}/HCO_3^-, which is also equal to the formation rate of $CO_3^{-\bullet}$, is $R_{CO_3^{-\bullet}} = 0.98$ $R_{\bullet_{OH}}$. Carbonate radicals react with either tyrosine or APAP, and the second-order reaction rate constant between tyrosine and $CO_3^{-\bullet}$ under ~neutral conditions is $k_{Tyr,CO_3^{-\bullet}} = 4.5 \cdot 10^7$ M^{-1} s^{-1} (Neta et al., 1988). The reaction rate between tyrosine and $CO_3^{-\bullet}$ is given by $R_{CO_3^{-\bullet}}$ times the fraction of $CO_3^{-\bullet}$ that reacts with tyrosine, and a similar issue holds for APAP. One obtains the following equations for the $CO_3^{-\bullet}$ reaction rates (remember that [Tyr] = [APAP] = 10 μM, and note that $R_{CO_3^{-\bullet}} = 0.98$ $R_{\bullet_{OH}}$):

$$R_{CO_3^{-\bullet}}^{Tyr} = R_{CO_3^{-\bullet}} \frac{k_{Tyr,CO_3^{-\bullet}}[CO_3^{-\bullet}][Tyr]}{k_{Tyr,CO_3^{-\bullet}}[CO_3^{-\bullet}][Tyr] + k_{APAP,CO_3^{-\bullet}}[CO_3^{-\bullet}][APAP]} = R_{CO_3^{-\bullet}} \frac{k_{Tyr,CO_3^{-\bullet}}}{k_{Tyr,CO_3^{-\bullet}} + k_{APAP,CO_3^{-\bullet}}} \quad (1)$$

$$R_{CO_3^{-\bullet}}^{APAP} = R_{CO_3^{-\bullet}} \frac{k_{APAP,CO_3^{-\bullet}}}{k_{Tyr,CO_3^{-\bullet}} + k_{APAP,CO_3^{-\bullet}}} \quad (2)$$

The degradation rate of both APAP and tyrosine is the sum of the reaction rates with $^{\bullet}OH$ and $CO_3^{-\bullet}$, thus $R_{Tyr} = R_{\bullet_{OH}}^{Tyr} + R_{CO_3^{-\bullet}}^{Tyr}$ and $R_{APAP} = R_{\bullet_{OH}}^{APAP} + R_{CO_3^{-\bullet}}^{APAP}$. Because [Tyr] = [APAP], the ratio $\mathfrak{R}$ of the first-order rate constants of the two compounds (k_{APAP} k_{Tyr}^{-1}) is equal to the ratio of the respective rates (R_{APAP} R_{Tyr}^{-1}). From the above discussion (including $R_{\bullet_{OH}}^{Tyr} = 1.8 \cdot 10^{-2}$ $R_{\bullet_{OH}}$, $R_{\bullet_{OH}}^{APAP} = 2 \cdot 10^{-3}$ $R_{\bullet_{OH}}$, $R_{CO_3^{-\bullet}} = 0.98$ $R_{\bullet_{OH}}$ and $k_{Tyr,CO_3^{-\bullet}} = 4.5 \cdot 10^7$ M^{-1} s^{-1}) and with some equation rearrangements one obtains:

$$\Re = 7.17 \pm 1.81 = \frac{R_{\bullet OH}^{APAP} + R_{CO_3^{-\bullet}}^{APAP}}{R_{\bullet OH}^{Tyr} + R_{CO_3^{-\bullet}}^{Tyr}} = \frac{2 \cdot 10^{-3} k_{Tyr,CO_3^{-\bullet}} + 0.982\, k_{APAP,CO_3^{-\bullet}}}{1.8 \cdot 10^{-2} k_{APAP,CO_3^{-\bullet}} + 0.998 k_{Tyr,CO_3^{-\bullet}}} \quad (3)$$

from which one finally gets $k_{APAP,CO_3^{-\bullet}} = (3.8\pm1.1)\cdot10^8\ \mathrm{M}^{-1}\ \mathrm{s}^{-1}$.

3.2. Photoinduced formation of intermediates

3.2.1. Quantification of hydroquinone (HQ) formation yield

HQ has been previously reported as APAP transformation intermediate (Yang et al., 2009; Peuravuori, 2012) and it was detected and quantified in this study as well. The reaction with $^{\bullet}$OH radicals was the only pathway where HQ could be found. UVB irradiation of 0.1 mM APAP with 3 mM H_2O_2 as $^{\bullet}$OH source (see Figure S7 in SM) yielded $R_{APAP} = (6.85\pm0.19)\cdot10^{-9}\ \mathrm{M}\ \mathrm{s}^{-1}$ as APAP initial transformation rate and $R_{HQ} = (4.51\pm0.23)\cdot10^{-11}\ \mathrm{M}\ \mathrm{s}^{-1}$ as HQ initial formation rate. The formation yield of HQ from APAP upon reaction with $^{\bullet}$OH is $\eta_{HQ}^{\bullet OH} = R_{HQ}\,(R_{APAP})^{-1} = (6.58\pm0.52)\cdot10^{-3}$. The HQ yields in other photochemical pathways can be safely neglected.

3.2.2. LC-MS identification of APAP transformation products (TPs)

Analysis of samples taken from experiments with 1 mM initial APAP concentration *via* LC-ESI-QTOF/MS/MS in both positive and negative ionisation mode revealed the formation of several TPs (Figure 3). Chemical structures were proposed based on exact masses, observed fragmentation patterns (MS^n experiments) as well as by comparison to literature results. So far, a number of studies have investigated the formation of TPs during photolytic and photocatalytic degradation of APAP (*e.g.* TiO$_2$/UV or H$_2$O$_2$/UV). However, a comprehensive overview of TPs formed from direct and indirect photolysis pathways of APAP, relevant for surface waters, is still missing.

Direct photolysis experiments revealed first of all the formation of dihydroxy-APAP (TP183) and of dihydroxy-benzoquinone imine-APAP (TP181), with fragmentation patterns in agreement with those reported in the literature (Trovo et al., 2012; Vogna et al., 2002). To our knowledge no TPs formed during the direct photolysis of APAP have been reported to date, but it has been shown that APAP can be degraded *via* UVB irradiation, though only slowly under laboratory conditions (Peuravuori, 2012). The detection of APAP dimers and trimers (Figure 3) is consistent with the formation of phenoxy radicals (Rayne et al., 2009; Fehir et al., 2009; Bartesaghi et al., 2010). Under UVB irradiation, these radical species would probably be formed *via* photoinduced cleavage of the O-H phenolic bond rather than by photoionisation, as already reported (De Laurentiis et al., 2013b). The detection of dimers and trimers by direct photolysis and other processes (*vide infra*) is mechanistically useful. However, it might have limited environmental significance because it is connected with a relatively high APAP concentration (1 mM, to allow intermediate identification),

under which conditions the dimerisation of the phenoxy radicals is favoured over competitive reactions.

Three additional TPs were detected, namely TP157A, TP139B and TP139C. For TP157A ($C_6H_7NO_4$), the cleavage of CO_2 was observed in MS^2 experiments and it indicates the presence of a carboxylic acid moiety. The direct photolysis of APAP would produce cleavage of the acetaldehyde moiety as well as fission of the aromatic ring. Photolytic N-dealkylation has also been described for other compounds such as the herbicide fenuron or the anti-malarial drug hydroxyl-chloroquine (Mazzocchi et al., 1972; Saini et al., 2013). Furthermore, the photolytic cleavage of phenol moieties has recently been described for the sunscreen agent 2-phenylbenzimidazole-5-sulfonic acid (Ji et al., 2013). For TP139B and TP139C, the same exact masses but different retention times were observed (Table 2). Compared to APAP, the obtained sum formulae show a loss of one carbon atom. MS^2 experiments revealed the cleavage of C_2H_2O from TP139A, indicating that the acetaldehyde moiety might have remained unchanged. For TP139B no fragments could be obtained. No chemical structures could be proposed for TP139B/C and their elucidation would require further studies, *e.g.* by NMR.

Indirect photolysis experiments in the presence of **carbonate radicals** ($CO_3^{-\bullet}$, produced by irradiation of nitrate with excess bicarbonate at pH 8.5) revealed the formation of dihydroxy-benzoquinone imine-APAP (TP181) as well as APAP dimers and trimers. The latter TPs suggest the formation of phenoxy radicals from APAP + $CO_3^{-\bullet}$, *via* electron transfer or hydrogen abstraction. These results are in agreement with Busset et al. (2007), who also observed the formation of phenoxy radicals in the reaction of phenols with $CO_3^{-\bullet}$ *via* laser flash photolysis. Furthermore, the reaction of $CO_3^{-\bullet}$ with the herbicide fenuron primarily leads to a quinone imine derivative and to hydroxylation of the aromatic ring (Mazellier et al., 2007).

Similarly to direct photolysis and reaction with $CO_3^{-\bullet}$, formation of APAP dimers and trimers was observed when using **AQ2S** as triplet sensitiser (Sens*). This is in good agreement with recent results obtained by De Laurentiis et al. (2013a), who investigated the photochemical fate of phenol in the presence of irradiated AQ2S. The system AQ2S + phenol produces phenoxy radicals that then evolve into dihydroxybiphenyls and phenoxyphenols through dimerisation. Besides the formation of APAP dimers and trimers, hydroxy-APAP (TP167A) was detected, with fragmentation pattern in agreement with that reported by Trovo et al. (2012). Formation of hydroxyderivatives in the absence of free $^\bullet$OH (which is not generated by AQ2S under irradiation; Bedini et al., 2012) can be due to reaction of water or OH$^-$ with aromatic radical cations, or to evolution of adducts formed between H_2O and radiation-excited molecules (Bedini et al., 2012; De Laurentiis et al., 2012a). The difficulty to distinguish between the reactivity of free $^\bullet$OH radicals and that of other transient species is well known in different fields such as heterogeneous photocatalysis and the Fenton reaction (Lee et al., 2005; Bataineh et al., 2012; Santiago-Morales et al., 2013). The detection of several TPs with four to six carbon atoms (TP115, TP116, TP157A and TP157B) also suggests fission of the aromatic ring and/or cleavage of the acetamide moiety. Interestingly, TP157A and TP157B have the same exact mass but their retention times differ by

almost 10 min. One likely explanation might be that TP157A is formed *via* cleavage of the aromatic ring, whereas for TP157B the ring is still intact. TP116 is likely to be butenedioic acid, which is supported by the cleavage of CO_2 in MS^2 experiments. For TP115 the elimination of NH_3 and H_2O is observed in MS^n experiments, indicating the presence of a primary amide and of an alcohol group. TP115 might thus resemble an amino-hydroxy-dihydrofuranone, but NMR analysis would be necessary to finally confirm its chemical structure.

In contrast to the experiments described so far, no APAP dimers or trimers were observed with **hydroxyl radicals** ($^\bullet$OH, generated by irradiation of H_2O_2). OH-radicals can react with phenolic moieties, as present in acetaminophen, *via* one-electron oxidation, addition to the aromatic ring and H atom abstraction (Singh et al., 2009). It has been shown that OH-radical adducts (*via* formation of carbon-centered radical intermediates) can undergo acid- and base-catalysed H_2O elimination yielding phenoxy-radicals (Raghavan et al. 1980; Tripathi et al., 2004). Thus, the neutral pH used in our study is likely to favour the formation of stable OH-radical adducts as indicated by the observed TPs. Under more acidic or basic conditions however, phenoxy radical formation might also play a role in the fate of APAP. In total, the formation of seven different TPs was observed with $^\bullet$OH, the main ones being hydroxy-APAP (TP167B), dihydroxy-benzoquinone imine APAP (TP181) and dihydroxybenzoquinone imine (TP139A). The formation of these TPs is in good agreement with results reported for the degradation of APAP *via* UV/H_2O_2, UV/TiO_2 and photo-Fenton (Andreozzi et al., 2003; Dalmazio et al., 2008; Trovo et al., 2012). It should be noted that the retention time of the detected hydroxy-APAP (TP167B) differed from that formed with irradiated AQ2S (TP167A). This might be due to differences in the formation pathways of hydroxylated derivatives *via* free $^\bullet$OH attack or oxidation processes in aqueous medium. The formation of butenedionic acid (TP116) was also observed, coherently with reports of Yang et al. (2009) who degraded APAP by UV/H_2O_2. Interestingly, TP116 and TP115 were detected in the presence of both AQ2S and H_2O_2 under irradiation, respectively yielding ^{3}AQ2S* and $^\bullet$OH as the main reactive species. The occurrence of the same intermediates in different pathways is observed quite often (Vione et al., 2011; De Laurentiis et al., 2012a). In the case of triplet sensitisers and $^\bullet$OH, it supports the current views that irradiated organic matter can yield low-level hydroxylating species which simulate the reactivity of free $^\bullet$OH (Page et al., 2011).

The identified compounds reported in Figure 3 do not overlap with human metabolites (APAP glucuronide and 4-aminophenol; Santos et al., 2013) or the main TPs of APAP biodegradation, namely 4-aminophenol and HQ (Hu et al., 2013; Zhang et al., 2013). Although HQ could be formed *via* both photo- and biotransformation of APAP, the photochemical pathway would have low environmental importance because of low formation yield of HQ from APAP + $^\bullet$OH (see section 3.2.1) and limited significance of the $^\bullet$OH pathway for APAP transformation in surface waters (*vide infra*).

The results of APAP photodegradation experiments clearly highlight the complexity of the direct and indirect photolysis processes that would lead to the formation of TPs in environmental waters. Water chemical parameters such as DOM concentration would be crucial with regard not

only to photodegradation kinetics, but also to the formation of TPs. Interestingly, hydroxy-APAP has been identified upon irradiation of APAP in the presence of natural CDOM and nitrate (Peuravuori, 2012), and the results of the present work enable the assumption that it could be formed by both $^\bullet OH$ and $^3CDOM^*$. The latter pathway could be quite significant in environmental waters (*vide infra*).

Also note that many of the studied pathways and related TPs could also be found during oxidation processes for water treatment. Actually, several advanced oxidation processes (AOPs) such as catalysed ozonation, TiO_2 photocatalysis, photo-Fenton and sonication have been tested for the degradation of APAP at both laboratory and pilot plant scale (Skoumal et al., 2006; Duran et al., 2011; Miranda-Garcia et al., 2011; Xiao et al., 2013). In addition to the already reported agreement between our $^\bullet OH$-related intermediates and those found in AOPs, reactions with $CO_3^{-\bullet}$ could be relevant to systems that generate $^\bullet OH$ in the presence of inorganic carbon (Canonica and Tratnyek, 2003). Furthermore, triplet sensitisers could be additional reactants when CDOM-containing waters are irradiated for treatment (Canonica et al., 2008). Direct photolysis in water treatment would usually take place under UVC, and care should be taken in extending UVB data to UVC conditions. Indeed, APAP has a 240-nm absorption band that would be excited by typical 254-nm UVC irradiation, while the photochemical behaviour under UVB would be rather the result of excitation of a shoulder band around 285 nm. Different absorption bands might be characterised by different photolysis quantum yields and they could yield different TPs when excited (Fischer and Warneck, 1996; Chawada et al., 2004).

3.3. Photochemical modelling of APAP transformation

Based on the data of APAP photochemical reactivity reported in Table 1, it is possible to model the photochemical transformation kinetics of APAP as a function of water chemistry and depth. Preliminary model calculations showed that reactions with $^\bullet OH$ and $^1O_2$ would play a minor role in APAP photodegradation. The main pathways would involve reaction with $CO_3^{-\bullet}$, $^3CDOM^*$ and the direct photolysis, the relative importance of which depends on environmental conditions. Formation of HQ from APAP + $^\bullet OH$ would have limited environmental importance and the relevant modelling is reported as SM. HQ can be detected in laboratory systems in the presence of APAP and of $^\bullet OH$ sources such as nitrate and H_2O_2 (Peuravuori, 2012 and this work). However, its importance as TP of APAP in the environment would be much lower, due to the presence of deeper water columns and of $^\bullet OH$ scavengers. Further issues are the relatively low reaction rate constant between APAP and $^\bullet OH$ (in the 10^9 M^{-1} s^{-1} range, while for many compounds it is an order of magnitude higher; Buxton et al., 1988) and the low formation yield of HQ from APAP + $^\bullet OH$ (below 1%).

3.3.1. APAP photodegradation
Figure 4a reports the modelled half-life time of APAP ($t_{1/2}^{APAP}$) as a function of the dissolved organic carbon (DOC) and the path length l of sunlight in water, which is proportional to the water depth d

(see section 2.7). The half-life time of APAP (average value in the water column of specified depth) would be in the range of one day to a couple of weeks, which implies that phototransformation in surface waters would be quite fast. Model results for low-l and low-DOC conditions are comparable with data obtained under laboratory irradiation (Yamamoto et al., 2009).

It is shown that $t_{1/2}^{APAP}$ increases with increasing l, mostly because the bottom layers of deeper water bodies are poorly illuminated by sunlight, which offsets the faster photoreactions in the upper layers. The trend with DOC shows a maximum around 5 mg C L^{-1}. This is accounted for by the fact that APAP degradation at low DOC would be prevalently carried out by direct photolysis and $CO_3^{-\bullet}$ reaction, while reaction with ^{3}CDOM* would prevail at high DOC.

The DOC effect on the $CO_3^{-\bullet}$ process is reported in Figure 4b, which considers pH ~ 8. The inhibition of $CO_3^{-\bullet}$ reactions is partially due to the fact that dissolved organic matter (DOM) scavenges $^\bullet$OH, inhibiting the production of $CO_3^{-\bullet}$ upon $^\bullet$OH-induced oxidation of carbonate and bicarbonate (Buxton et al., 1988). Another inhibition effect is linked with the direct consumption of $CO_3^{-\bullet}$ by DOM (Huang and Mabury, 2000; Canonica et al., 2005). Such an inhibition is not offset by oxidation of carbonate to $CO_3^{-\bullet}$ by ^{3}CDOM*, which is usually a secondary source of $CO_3^{-\bullet}$ in surface waters (Canonica et al., 2005; Vione et al., 2009b). The figure also shows that reaction with $CO_3^{-\bullet}$ would be very important for APAP photochemical transformation at DOC values below 3 mg C L^{-1}.

An important factor in the reactivity of $CO_3^{-\bullet}$ is represented by the effect of pH. The main pathway of $CO_3^{-\bullet}$ production in surface waters is the oxidation of carbonate and bicarbonate by $^\bullet$OH (Huang and Mabury, 2000; Canonica et al., 2005). Because carbonate is about 50 times more reactive than bicarbonate with $^\bullet$OH (Buxton et al., 1988), the formation rate of $CO_3^{-\bullet}$ would increase with increasing pH. The pH trend of $CO_3^{-\bullet}$ formation due to the acid-base equilibria of inorganic carbon species is reported in SM (Figure S8). The effect of pH would be relatively limited in the 7-8 pH interval, considering that $CO_3^{-\bullet}$ formation rate at pH 8 would be only 40% faster than at pH 7. In fact, at 7 < pH < 8 bicarbonate would be both the main inorganic carbon species and the main precursor of $CO_3^{-\bullet}$. Interestingly, such pH conditions are very common in surface waters (Polesello et al., 2006).

At pH < 7 bicarbonate would account for a decreasing fraction of inorganic carbon, and CO_2 and carbonic acid are practically unreactive toward $^\bullet$OH (Buxton et al., 1988). As a consequence, compared with pH 7, the formation rate of $CO_3^{-\bullet}$ would be lower by ~2.5 times at pH 6, ~18 times at pH 5 and ~170 times at pH 4. At pH > 8 there would be a growing importance of carbonate as $CO_3^{-\bullet}$ source and, for instance, at pH 9 the formation rate of $CO_3^{-\bullet}$ would be ~2.5 times higher than at pH 8.

The modelled fraction of APAP that is degraded by direct photolysis (Figure 4c) decreases with increasing l and has a maximum as a function of DOC. The maximum with DOC depends on the competition for APAP degradation between $CO_3^{-\bullet}$, direct photolysis and ^{3}CDOM*. Organic matter inhibits both $CO_3^{-\bullet}$ reactions (as explained above) and the direct photolysis, the latter because of competition for sunlight irradiance between CDOM and APAP. The inhibition by DOM of $CO_3^{-\bullet}$

reactions would be more effective than the inhibition of direct photolysis, which explains the initial increase with DOC of the photolysis fraction. However, ^{3}CDOM* reactions are enhanced by organic matter and they would soon prevail over direct photolysis, the importance of which would decrease at high DOC. APAP direct photolysis would also become less important by increasing the path length l of sunlight, because photolysis is triggered by UVB radiation that penetrates little in the water column. In contrast, ^{3}CDOM* is generated by CDOM that also absorbs more penetrating UVA and visible radiation. Figure 4c additionally shows that direct photolysis would play a significant role in APAP transformation (up to 9% of the total) at around 3-6 mg C L^{-1} DOC.

Figure 5a shows that the fraction of APAP that is degraded by $CO_3^{-\bullet}$ would increase with both bicarbonate and nitrate. Indeed, a major process of $CO_3^{-\bullet}$ formation is the reaction of HCO_3^- with $^\bullet$OH, of which nitrate irradiation is one of the possible photochemical sources.

The importance of APAP degradation by ^{3}CDOM* depends on the rate constant $k_{APAP,^3CDOM*}$. The main problem is that CDOM is a mixture of thousands of compounds with different properties (Peuravuori and Pihlaja, 1997), which makes it very difficult to measure a second-order reaction rate constant. Therefore, one may be obliged to follow the potentially problematic path of using probe molecules such as AQ2S. The second-order rate constant here determined might be representative of the CDOM triplet states that are most reactive with APAP. Average ^{3}CDOM* might be less reactive than ^{3}AQ2S*, which prompts for the modelling of $t_{1/2}^{APAP}$ with different values of $k_{APAP,^3CDOM*}$. This is easily allowed by the APEX software and Figure 5b reports the modelled $t_{1/2}^{APAP}$ as a function of DOC and $k_{APAP,^3CDOM*}$ (the latter varied in the range of 10^8-10^{10} M^{-1} s^{-1}). No change of $t_{1/2}^{APAP}$ with $k_{APAP,^3CDOM*}$ can be observed at low DOC, where reaction with $CO_3^{-\bullet}$ and the direct photolysis would mostly account for APAP transformation. Conversely, $t_{1/2}^{APAP}$ decreases with increasing $k_{APAP,^3CDOM*}$ at high DOC, where reaction with ^{3}CDOM* could predominate. Moreover, if $k_{APAP,^3CDOM*}$ is low, $t_{1/2}^{APAP}$ increases with DOC because of the inhibition of direct photolysis and $CO_3^{-\bullet}$ reaction. Coherently with this trend, a possible explanation for the discrepancy between APAP photodegradation kinetics reported by Peuravuori (2012) and by Yamamoto et al. (2009) is that the lower rates in the former case (APAP irradiation in lake water) might be associated with the occurrence of an elevated amount of organic matter (up to 40 mg C L^{-1} DOC) with limited ability to sensitise APAP transformation.

The value of $k_{APAP,^3CDOM*}$ could vary considerably in different environments, as allochthonous CDOM from soil is usually more photoactive than aquagenic, proteinaceous CDOM or CDOM derived from atmospheric deposition (De Laurentiis et al., 2012b). However, $t_{1/2}^{APAP}$ would be practically independent of $k_{APAP,^3CDOM*}$ for DOC < 2 mg C L^{-1}, while a strong dependence on $k_{APAP,^3CDOM*}$ could be expected for DOC > 5 mg C L^{-1} (see Figure S9 in SM).

The values of the photochemical $t_{1/2}^{APAP}$ (days to several weeks depending on conditions) are in the same range as those reported for biodegradation (Yamamoto et al., 2009; Lin et al., 2010). Both photochemical and biological processes could thus be important in APAP removal from surface waters.

3.3.2. Model uncertainty and seasonal trends

Model uncertainty can be assessed with the *APEX_Errors* function of the APEX software. If one considers for instance a water body with 5 m depth, 3 mg C L^{-1} DOC, 0.1 mM nitrate, 1 µM nitrite, 1 mM bicarbonate and 10 µM carbonate, from the model one gets $t_{1/2}^{APAP}$ = 4.4±2.0 SSD (µ±σ). An uncertainty of ~45% is quite representative of model predictions for APAP, combining uncertainty on both experimental rate constants (see Table 1) and empirical parameters of model equations.

Model predictions are valid for summertime conditions at mid latitude. An approximate assessment of the mid-latitude seasonal trend can be obtained with the *APEX_Season* function. With the water conditions reported above, $t_{1/2}^{APAP}$ would vary from 4.3 days in June to 23-35 days in December-January.

4. Conclusions

- The main phototransformation pathways of APAP in surface waters would be direct photolysis and reaction with $CO_3^{-\bullet}$ and possibly $^3CDOM^*$. The latter process would be unimportant below 2 mg C L^{-1} DOC. The importance of the reaction between APAP and $CO_3^{-\bullet}$ would increase with increasing pH, especially outside the pH interval 7-8. Inside that interval the pH effect is less marked, because bicarbonate is both the main inorganic carbon species and the main source of $CO_3^{-\bullet}$ by reaction with $^\bullet OH$. In the pH range 7-8, which is quite common in surface waters, reaction with $CO_3^{-\bullet}$ is expected to be the predominant APAP phototransformation pathway for DOC < 3 mg C L^{-1} and for nitrate and bicarbonate levels around 10^{-4} and 10^{-3} M, respectively. Under favourable conditions (3-6 mg C L^{-1} DOC), direct photolysis could account for up to 9% of APAP transformation. The $CO_3^{-\bullet}$ process has been largely neglected so far, which suggests that APAP phototransformation in surface waters could be more important than commonly assumed. The photochemical half-life time of APAP has potentially high variability (in the day-month range) depending on environmental conditions, including seasonality. In the most favourable cases, APAP phototransformation could be comparable to or more important than biological degradation in surface-water environments.
- There is a large overlap between TPs formed *via* several pathways, many of which might involve phenoxy radicals as reaction intermediates. By considering only the photoprocesses of highest environmental importance (photolysis and reaction with $CO_3^{-\bullet}$ and $^3CDOM^*$), one can hypothesise significant formation of hydroxylated derivatives (probably through oxidation-hydroxylation, which would simulate the reactivity of free $^\bullet OH$), ring-opening compounds and (at APAP concentration values significantly higher than typical environmental ones) dimers and trimers. Triplet-sensitised transformation might also yield ring-rearrangement compounds characterised by the presence of five-member rings. These structures need additional confirmation because they could be markers of triplet-sensitised APAP transformation under high-DOC conditions.

- There seems to be limited or no overlap between the photochemical TPs detected in this work and those derived from APAP biological degradation or human metabolism. Therefore, the compounds shown in Figure 3 could be used as markers of APAP phototransformation in surface waters.

References

Andreozzi, R., Caprio, V., Marotta, R., Vogna, D., 2003. Paracetamol oxidation from aqueous solutions by means of ozonation and H_2O_2/UV system. Water Research 37, 993-1004.

Bartesaghi, S., Wenzel, J., Trujillo, M., Lopez, M., Joseph, J., Kalyanaraman, B., Radi, R., 2010. Lipid peroxyl radicals mediate tyrosine dimerization and nitration in membranes. Chemical Research in Toxicology 23, 821-835.

Bataineh, H., Pestovsky, O., Bakac, A., 2012. pH-induced mechanistic changeover from hydroxyl radicals to iron(IV) in the Fenton reaction. Chemical Science 3, 1594-1599.

Bedini, A., De Laurentiis, E., Sur, B., Maurino, V., Minero, C., Brigante, M., Mailhot, G., Vione, D., 2012. Phototransformation of anthraquinone-2-sulphonate in aqueous solution. Photochemical and Photobiological Sciences 11, 1445-1453.

Boreen, A. L., Arnold, W. A., McNeill, K., 2003. Photodegradation of pharmaceuticals in the aquatic environment: A review. Aquatic Sciences 65, 320-341.

Brigante, M., Charbouillot, T., Vione, D., Mailhot, G., 2010. Photochemistry of 1-nitronaphthalene: A potential source of singlet oxygen and radical species in atmospheric waters. Journal of Physical Chemistry A 114, 2830-2836.

Buxton, G.V., Greenstock, C.L., Helman, W.P., Ross, A.B., 1988. Critical review of rate constants for reactions of hydrated electrons, hydrogen atoms and hydroxyl radicals ($^\bullet$OH/O$^{-\bullet}$) in aqueous solution. Journal of Physical and Chemical Reference Data 17, 1027-1284.

Canonica, S., Tratnyek, P. G., 2003. Quantitative structure-activity relationships for oxidation reactions of organic chemicals in water. Environmental Toxicology and Chemistry 22, 1743-1754.

Canonica, S., Kohn, T., Mac, M., Real, F.J., Wirz, J., Von Gunten, U., 2005. Photosensitizer method to determine rate constants for the reaction of carbonate radical with organic compounds. Environmental Science and Technology 39, 9182-9188.

Canonica, S., Hellrung, B., Müller, P., Wirz, J., 2006. Aqueous oxidation of phenylurea herbicides by triplet aromatic ketones. Environmental Science & Technology 40, 6636-6641.

Canonica, S., Meunier, L., Von Gunten, U., 2008. Phototransformation of selected pharmaceuticals during UV treatment of drinking water. Water Research 42, 121-128.

Chawada, S. S., Ameta, S. C., Jain, S., 2004. Wavelength-dependent phototransformation of dibenzylideneacetonedibromide. Journal of the Indian Chemical Society 81, 965-967.

Chiron, S., Gomez, E., Fenet, H., 2010. Nitration processes of acetaminophen in nitrifying activated sludge. Environmental Science and Technology 44, 284-289.

Cory, R. M., McKnight, D. M., 2005. Fluorescence spectroscopy reveals ubiquitous presence of oxidized and reduced quinones in dissolved organic matter. Environmental Science and Technology 39, 8142-8149.

Dalmazio, I., Alves, T.M.A., Augusti, R., 2008. An appraisal on the degradation of paracetamol by TiO_2/UV system in aqueous medium. Product identification by gas chromatography-mass spectrometry (GC-MS). Journal of the Brazilian Chemical Society 19, 81-88.

De Laurentiis, E., Chiron, S., Kouras-Hadef, S., Richard, C., Minella, M., Maurino, V., Minero, C., Vione, D., 2012a. Photochemical fate of carbamazepine in surface freshwaters: Laboratory measures and modelling. Environmental Science and Technology 46, 8164-8173.

De Laurentiis, E., Minella, M., Maurino, V., Minero, C., Brigante, M., Mailhot, G., Vione, D., 2012b. Photochemical production of organic matter triplet states in water samples from mountain lakes, located below or above the tree line. Chemosphere 88, 1208–1213.

De Laurentiis, E., Maurino, V., Minero, C., Vione, D., Mailhot, G., Brigante, M., 2013a. Could triplet-sensitised transformation of phenolic compounds represent a source of fulvic-like substances in natural waters? Chemosphere 90, 881-884.

De Laurentiis, E., Minella, M., Sarakha, M., Marrese, A., Minero, C., Mailhot, G., Brigante, M., Vione, D., 2013b. Photochemical processes involving the UV absorber benzophenone-4 (2-hydroxy-4-methoxybenzophenone-5-sulphonic acid) in aqueous solution: Reaction pathways and implications for surface waters. Water Research 47, 5943-5953.

Del Rio, H., Suarez, J., Puertas, J., Ures, P., 2013. PPCPs wet weather mobilization in a combined sewer in NW Spain. Science of the Total Environment 449, 189-198.

Donner, E., Kosjek, T., Qualmann, S., Kusk, K. O., Heath, E., Revitt, D. M., Ledin, A., Andersen, H. R., 2013. Ecotoxicity of carbamazepine and its UV photolysis transformation products. Science of the Total Environment 443, 870-876.

Duran, A., Monteagudo, J. M., Carnicer, A., Ruiz-Murillo, M., 2011. Photo-Fenton mineralization of synthetic municipal wastewater effluent containing acetaminophen in a pilot plant. Desalination 270, 124-129.

EFPIA (European Federation of Pharmaceutical Industries and Associations), 2006. The Pharmaceutical Industry in Figures. EFPIA press, Brussels, 49 pp.

Fehir, R.J.Jr., McCusker, J.K., 2009. Differential polarization of spin and charge density in substituted phenoxy radicals. Journal of Physical Chemistry A 113, 9249-9260.

Fischer, M., Warneck, P., 1996. Photodecomposition of nitrite and undissociated nitrous acid in aqueous solution. Journal of Physical Chemistry 100, 18749-18756.

Gerecke, A. C., Canonica, S., Müller, S. R., Scharer, M., Schwarzenbach, R. P., 2001. Quantification of dissolved natural organic matter (DOM)-mediated phototransformation of phenylurea herbicides in lakes. Environmental Science and Technology 35, 3915-3923.

Gros, M., Petrovíc, M., Ginebreda, A., Barceló, D., 2010. Removal of pharmaceuticals during wastewater treatment and environmental risk assessment using hazard indexes. Environment International 36, 15-26.

Hari, A. C., Paruchuri, R. A., Sabatini, D. A., Kibbey, T. C. G., 2005. Effects of pH and cationic and nonionic surfactants on the adsorption of pharmaceuticals to a natural aquifer material. Environmental Science and Technology 39, 2592-2598.

Hu, J., Zhang, L. L., Chen, J. M., Liu, Y., 2013. Degradation of paracetamol by Pseudomonas aeruginosa strain HJ1012. Journal of Environmental Science and Health Part A 48, 791-799.

Huang, J. P., Mabury, S. A., 2000. Steady-state concentrations of carbonate radicals in field waters. Environmental Toxicology and Chemistry 19, 2181-2188.

Jones, O.A.H., Voulvoulis, N., Lester, J. N., 2002. Aquatic environmental assessment of the top 25 English prescription pharmaceuticals. Water Research 36, 5013–5022.

Ji, Y., Zhou, L., Zhang, Y., Ferronato, C., Brigante, M., Mailhot, G., Yang, X., Chovelon, J.-M., 2013. Photochemical degradation of sunscreen agent 2- phenylbenzimidazole-5-sulfonic acid in different water matrices. Water Research 47, 5865-5875.

Jones, O.A.H., Voulvoulis, N., Lester, J. N., 2005. Human pharmaceuticals in wastewater treatment processes. Critical Reviews in Environmental Science and Technology 35, 401-427.

Kliegman, S., Eustis, S. N., Arnold, W. A., McNeill, K., 2013. Experimental and theoretical insights into the involvement of radicals in triclosan phototransformation. Environmental Science and Technology 47, 6756-6763.

Lee, J., Choi, W. Y., Yoon, J., 2005. Photocatalytic degradation of N-nitrosodimethylamine: Mechanism, product distribution, and TiO_2 surface modification. Environmental Science and Technology 39, 6800-6807.

Loffler, D., Rombke, J., Meller, M., Ternes, T. A., 2005. Environmental fate of pharmaceuticals in water/sediment systems. Environmental Science and Technology 39, 5209-5218.

Maddigapu, P. R., Bedini, A., Minero, C., Maurino, V., Vione, D., Brigante, M., Mailhot, G., Sarakha, M., 2010. The pH-dependent photochemistry of anthraquinone-2-sulfonate. Photochemical and Photobiological Sciences 9, 323-330.

Mazellier, P., Busset, C., Delmont, A., De Laat, J., 2007, A comparison of fenuron degradation by hydroxyl and carbonate radicals in aqueous solution. Water Research 41, 4585-4594.

Mazzocchi, P.H., Rao, M.P., 1972. Photolysis of 3-(para-chlorophenyl)-1,1-dimethylurea (Monuron) and 3-phenyl-1,1-dimethylurea (Fenuron). Journal of Agricultural and Food Chemistry 20, 957-959.

McBride, J. T., 2011. The association of acetaminophen and asthma prevalence and severity. Pediatrics 128, 1181-1185.

Minella, M., Romeo, F., Vione, D., Maurino, V., Minero, C., 2011. Low to negligible photoactivity of lake-water matter in the size range from 0.1 to 5 µm. Chemosphere 83, 1480-1485.

Minella, M., De Laurentiis, E., Buhvestova, O., Haldna, M., Kangur, K., Maurino, V., Minero, C., Vione, D., 2013. Modelling lake-water photochemistry: Three-decade assessment of the steady-state concentration of photoreactive transients ($^{\bullet}OH$, $CO_3^{-\bullet}$ and $^3CDOM^*$) in the surface water of polymictic Lake Peipsi (Estonia/Russia). Chemosphere 90, 2589-2596.

Miranda-Garcia, N., Suarez, S., Sanchez, B., Coronado, J. M., Malato, S., Maldonado, M. I., 2011. Photocatalytic degradation of emerging contaminants in municipal wastewater treatment plant effluents using immobilized TiO_2 in a solar pilot plant. Applied Catalysis B: Environmental 103, 294-301.

Morasch, B., Bonvin, F., Reiser, H., Grandjean, D., de Alencastro, L. F., Perazzolo, C., Chevre, N., Kohn, T., 2010. Occurrence and fate of micropollutants in the Vidy Bay of Lake Geneva, Switzerland. Part II: Micropollutant removal between wastewater and raw drinking water. Environmental Toxicology and Chemistry 29, 1658-1668.

Neta, P., Huie, R. E., Ross, A. B., 1988. Rate constants for reactions of inorganic radicals in aqueous solution, Journal of Physical and Chemical Reference Data 17, 1027-1034.

Newson, R. B., Shaheen, S. O., Chinn, S., Burney, P. G. J., 2000. Paracetamol sales and atopic disease in children and adults: an ecological analysis. European Respiratory Journal 16, 817-823.

Page, S. E., Arnold, W. A., McNeill, K., 2011. Assessing the contribution of free hydroxyl radical in organic matter-sensitized photohydroxylation reactions. Environmental Science and Technology 45, 2818-2825.

Peuravuori, J., Pihlaja, K., 1997. Molecular size distribution and spectroscopic properties of aquatic humic substances. Analytica Chimica Acta 337, 133-149.

Peuravuori, J., 2012. Aquatic photochemistry of paracetamol in the presence of dissolved organic chromophoric material and nitrate. Environmental Science and Pollution Research 19, 2259–2270.

Polesello, S., Tartari, G., Giacomotti, P., Mosello, R., Cavalli, S., 2006. Determination of total dissolved inorganic carbon in freshwaters by reagent-free ion chromatography. Journal of Chromatography A 1118, 56-61.

Raghavan, N.V., Steenken, S., 1980. Electrophilic reaction of the OH radical with phenol. Determination of the distribution of isomeric dihydroxycyclohexadienyl radicals. Journal of the American Chemical Society 102, 3495-3499.

Rayne, S., Forest, K., Friesen, K.J., 2009. Mechanistic aspects regarding the direct aqueous environmental photochemistry of phenol and its simple halogenated derivatives. A review. Environment International, 35, 425-437.

Ruggeri, G., Ghigo, G., Maurino, V., Minero, C., Vione, D., 2013. Photochemical transformation of ibuprofen into harmful 4-isobutylacetophenone: Pathways, kinetics, and significance for surface waters. Water Research 47, 6109-6121.

Saini, B., Bansal, G.; 2013. Characterization of four new photodegradation products of hydroxychloroquine through LC-PDA, ESI-MSn and LC-MS-TOF studies. Journal of Pharmaceutical and Biomedical Analysis 84, 224-231.

Santiago-Morales, J., Aguera, A., Gomez, M. D., Fernandez-Alba, A. R., Gimenez, J., Esplugas, S., Rosal, R., 2013. Transformation products and reaction kinetics in simulated solar light photocatalytic degradation of propranolol using Ce-doped TiO_2. Applied Catalysis B: Environmental 129, 13-29.

Santos, L. H. M. L. M., Paiga, P., Araujo, A. N., Pena, A., Delerue-Matos, C., Montenegro, M. C. B. S. M., 2013. Development of a simple analytical method for the simultaneous determination of paracetamol, paracetamol-glucuronide and p-aminophenol in river water. Journal of Chromatography B 930, 75-81.

Singh, U., Barik, A., Priyadarsini, I., 2009. Reactions of hydroxyl radical with bergenin, a natural poly phenol studied by pulse radiolysis. Bioorganic & Medical Chemistry 17, 6008-6014.

Skoumal, M., Cabot, P. L., Centellas, F., Arias, C., Rodriguez, R. M., Garrido, J. A., Brillas, E., 2006. Mineralization of paracetamol by ozonation catalyzed with Fe^{2+}, Cu^{2+} and UVA light. Applied Catalysis B: Environmental 66, 228-240.

Stamatis, N. K., Konstantinou, I. K., 2013. Occurrence and removal of emerging pharmaceutical, personal care compounds and caffeine tracer in municipal sewage treatment plant in Western Greece. Journal of Environmental Science and Health. Part B, Pesticides, Food Contaminants, and Agricultural Wastes 48, 800-813.

Tixier, C., Singer, H. P., Oellers, S., Müller, S. R., 2003. Occurrence and fate of carbamazepine, clofibric acid, diclofenac, ibuprofen, ketoprofen, and naproxen in surface waters. Environmental Science and Technology 37, 1061-1068.

Tripathi, G.N.R., Su, Y., 2004. The origin of base catalysis in the $^\bullet OH$ oxidation of phenols in water. Journal of Physical Chemistry A 108, 3478-3484.

Trovo, A.G., Nogueira, R.F.P., Aguera, A., Fernandez-Alba, A.R., Malato, S., 2012. Paracetamol degradation intermediates and toxicity during photo-Fenton treatment using different iron species. Water Research 46, 5374-5380.

Vione, D., Khanra, S., Cucu Man, S., Maddigapu, P. R., Das, R., Arsene, C., Olariu, R. I., Maurino, V., Minero, C., 2009a. Inhibition vs. enhancement of the nitrate-induced phototransformation of organic substrates by the $^\bullet OH$ scavengers bicarbonate and carbonate. Water Research 43, 4718-4728.

Vione, D., Maurino, V., Minero, C., Carlotti, M. E., Chiron, S., Barbati, S., 2009. Modelling the occurrence and reactivity of the carbonate radical in surface freshwater. Comptes Rendus Chimie 12, 865-871.

Vione, D., Maddigapu, P. R., De Laurentiis, E., Minella, M., Pazzi, M., Maurino, V., Minero, C., Kouras, S., Richard, C., 2011. Modelling the photochemical fate of ibuprofen in surface waters. Water Research 45, 6725-6736.

Vogna, D., Marotta, R., Napolitano, A., d'Ischia, M., 2002. Advanced oxidation chemistry of paracetamol. UV/H_2O_2-induced hydroxylation/degradation pathways and ^{15}N-aided inventory of nitrogenous breakdown products. Journal of Organic Chemistry 67, 6143-6151.

Weeks, J. L., Rabani, J., 1966. The pulse radiolysis of deaerated aqueous carbonate solutions. I. Transient optical spectrum and mechanism. II. pK for OH radicals. Journal of Physical Chemistry 70, 2100-2106.

Xiao, R. Y., Diaz-Rivera, D., Weavers, L. K., 2013. Factors influencing pharmaceutical and personal care product degradation in aqueous solution using pulsed wave ultrasound. Industrial & Engineering Chemistry Research 52, 2824-2831.

Yamamoto, H., Hayashi, A., Nakamura, Y., Sekizawa, J., 2005. Fate and partitioning of selected pharmaceuticals in the aquatic environment. Environmantal Science 12, 347–358.

Yamamoto, H., Nakamura, Y., Moriguchi, S., Nakamura, Y., Honda, Y., Tamura, I., Hirata, Y., Hayashi, A., Sekizawa, J., 2009. Persistence and partitioning of eight selected pharmaceuticals in the aquatic environment: Laboratory photolysis, biodegradation, and sorption experiments. Water Research 43, 351-362.

Yang, L., Yu, L. E., Ray, M. B., 2009. Photocatalytic oxidation of paracetamol: Dominant reactants, intermediates, and reaction mechanisms. Environmental Science and Technology 43, 460-465.

Zhang, L. L., Hu, J., Zhu, R. Y., Zhou, Q. W., Chen, J. M., 2013. Degradation of paracetamol by pure bacterial cultures and their microbial consortium. Applied Microbiology and Biotechnology 97, 3687-3698.

Table 1. Photochemical reactivity parameters of APAP (direct photolysis quantum yield and reaction rate constants with $^\bullet OH$, $CO_3^{-\bullet}$, $^1O_2$ and $^3AQ2S^*$, the latter as proxy of $^3CDOM^*$). The direct photolysis quantum yield obtained in this work is within the (relatively wide) range of values reported in the literature (Yamamoto et al., 2009). The reaction rate constant with $^\bullet OH$ is in good agreement with Yang et al. (2009).

Parameter	Value (μ±σ)
Φ_{APAP}	$(4.57\pm0.17)\cdot10^{-2}$
$k_{^\bullet OH,APAP}$	$(1.87\pm0.56)\cdot10^9\ M^{-1}\ s^{-1}$
$k_{CO_3^{-\bullet},APAP}$	$(3.8\pm1.1)\cdot10^8\ M^{-1}\ s^{-1}$
$k_{^1O_2,APAP}$	$(3.68\pm0.73)\cdot10^7\ M^{-1}\ s^{-1}$
$k_{^3CDOM^*,APAP}$	$(1.08\pm0.16)\cdot10^{10}\ M^{-1}\ s^{-1}$

Table 2. Detected TPs during direct and indirect photolysis experiments. The table reports retention times, exact masses (fragments included) and sum formula in both negative and positive ESI-mode.

Irradiation experiment	ESI mode	Acronym	RT [min]	Exact mass	Sum formula	Δ [ppm]
−	negative	**APAP**	17.9	150.0563	$C_8H_8NO_2$	1.7
				107.0378	C_6H_5NO	1.3
	positive	**APAP**	17.9	152.0706	$C_8H_{10}NO_2$	0.0
				134.0603	C_8H_8NO	1.9
				110.0604	C_6H_8NO	6.9
				93.1035	C_6H_5O	15.1
				92.0505	C_6H_6N	11.1
				82.0663	C_5H_8N	14.3
Direct photolysis (°)	negative	**TP157A**	6.5	156.0292	$C_6H_6NO_4$	-6.6
				112.0400	$C_5H_6NO_2$	-3.6
				70.0312	C_3H_4NO	19.5
		TP139B	16.4	138.0552	$C_7H_8NO_2$	-6.2
				96.0454	C_5H_6NO	-0.9
		TP139C	17.9	138.0563	$C_7H_8NO_2$	1.8
				-		
		TP181	20.5	180.0301	$C_8H_6NO_4$	-0.7
				138.0198	$C_6H_4NO_2$	1.0
				110.0251	$C_5H_4NO_2$	2.1
	positive	**TP183**	16.4	184.0597	$C_8H_{10}NO_4$	-0.4
				166.0488	$C_8H_8NO_3$	-6.4
				124.0389	$C_6H_6NO_2$	-3.3
				68.0509	C_4H_6N	20.9
Nitrate + bicarbonate ($CO_3^{-\bullet}$) (°)	negative	**TP181**	20.5	180.0288	$C_8H_6NO_4$	-8.0
				138.0198	$C_6H_4NO_2$	1.0
				110.0251	$C_5H_4NO_2$	2.1
Irradiated AQ2S (Sens*) (°)	negative	**TP116**	4.4	115.0039	$C_4H_3O_4$	1.9
				71.0138	$C_3H_3O_2$	0.4
		TP157A	6.5	156.0304	$C_6H_6NO_4$	1.1
				112.0400	$C_5H_6NO_2$	-3.6
				70.0312	C_3H_4NO	19.5
		TP167A	15.7	166.0513	$C_8H_8NO_3$	-6.4
				-		
		TP157B	16.9	156.0304	$C_6H_6NO_4$	1.1
				-		
	positive	**TP115**	6.4	116.0340	$C_4H_6NO_3$	-1.9
				99.0082	$C_4H_3O_3$	5.3
				98.0238	$C_4H_4NO_2$	1.5
		TP167A	15.7	168.0647	$C_8H_{10}NO_3$	-5.5
				126.0555	$C_6H_8NO_2$	4.3
				108.0446	C_6H_6NO	1.9
				80.0509	C_5H_6N	17.8
H_2O_2 ($^\bullet OH$)	negative	**TP116**	4.4	115.0043	$C_4H_3O_4$	5.4
				71.0417	$C_3H_3O_2$	11.9
		TP113	6.5	112.0409	$C_5H_6NO_2$	14.2

		-			
	TP167B	16.5	166.0511	$C_8H_8NO_3$	3.2
			124.0404	$C_6H_6NO_2$	0.8
			109.0168	$C_5H_3NO_2$	-1.2
			52.0202	C_3H_2N	17.8
	TP181	20.5	180.0304	$C_8H_6NO_4$	0.9
			138.0198	$C_6H_4NO_2$	1.0
			110.0251	$C_5H_4NO_2$	2.1
	TP115B	6.4	116.0327	$C_4H_6NO_3$	-13.1
			98.0235	$C_4H_4NO_2$	-3.6
positive	**TP167B**	16.5	168.0643	$C_8H_{10}NO_3$	-7.3
			126.0549	$C_6H_8NO_2$	-0.4
			109.0285	$C_6H_5O_2$	0.9
			108.0443	C_6H_6NO	-0.8
			81.0346	C_5H_5O	13.7
	TP139A	20.4	140.0336	$C_6H_6NO_3$	-4.4
			112.0396	$C_5H_6NO_2$	2.6

- no fragments detected in MS/MS experiments
(°) formation of APAP dimers and trimers observed
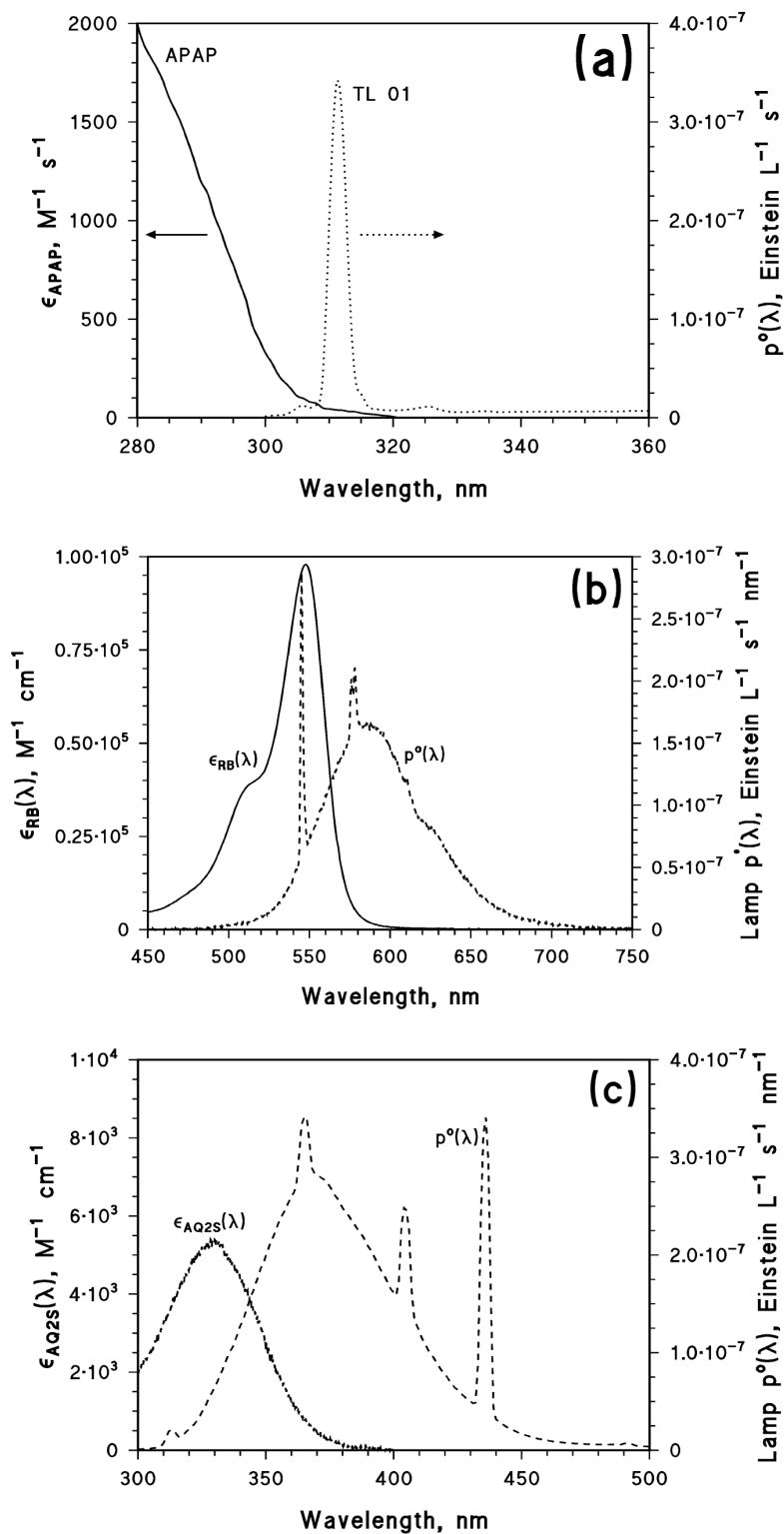
Figure 1. (a) APAP absorption spectrum (molar extinction coefficient) and emission spectrum of the UVB lamp (incident spectral photon flux density, measured with an Ocean Optics USB 2000 CCD spectrophotometer and normalised to actinometry data).

(b) Absorption spectrum of Rose Bengal (RB) and emission spectrum of the yellow lamp.

(c) Absorption spectrum of AQ2S and emission spectrum of the UVA lamp.
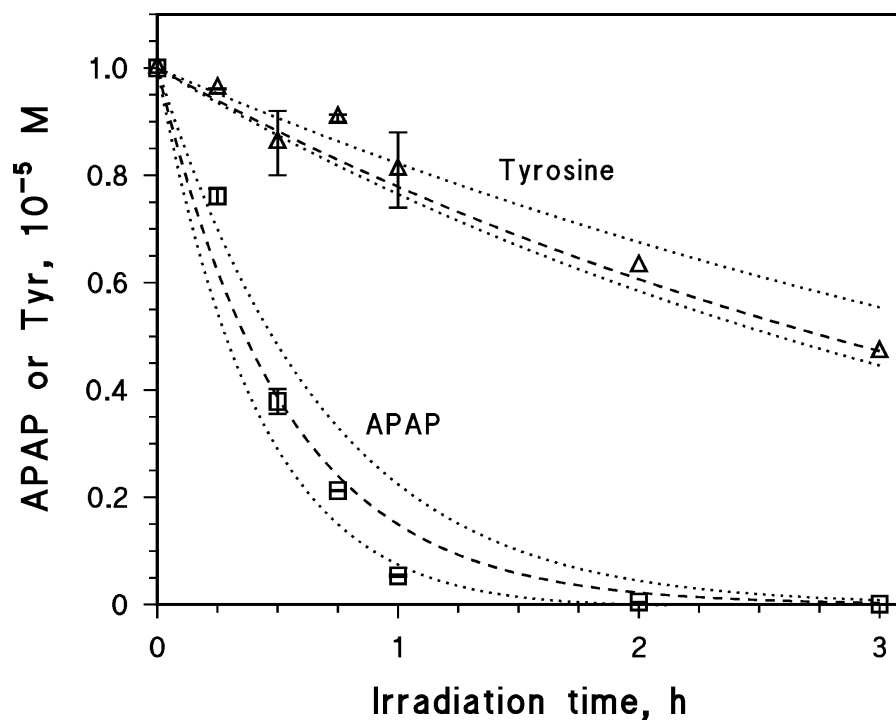
Figure 2. Time trend of APAP and tyrosine (10 μM initial concentration for both) upon UVB irradiation of 0.01 M NaNO$_3$ + 0.10 M NaHCO$_3$ (pH 8.2). Fit curves are dashed, 95% confidence bands of the fit are dotted.
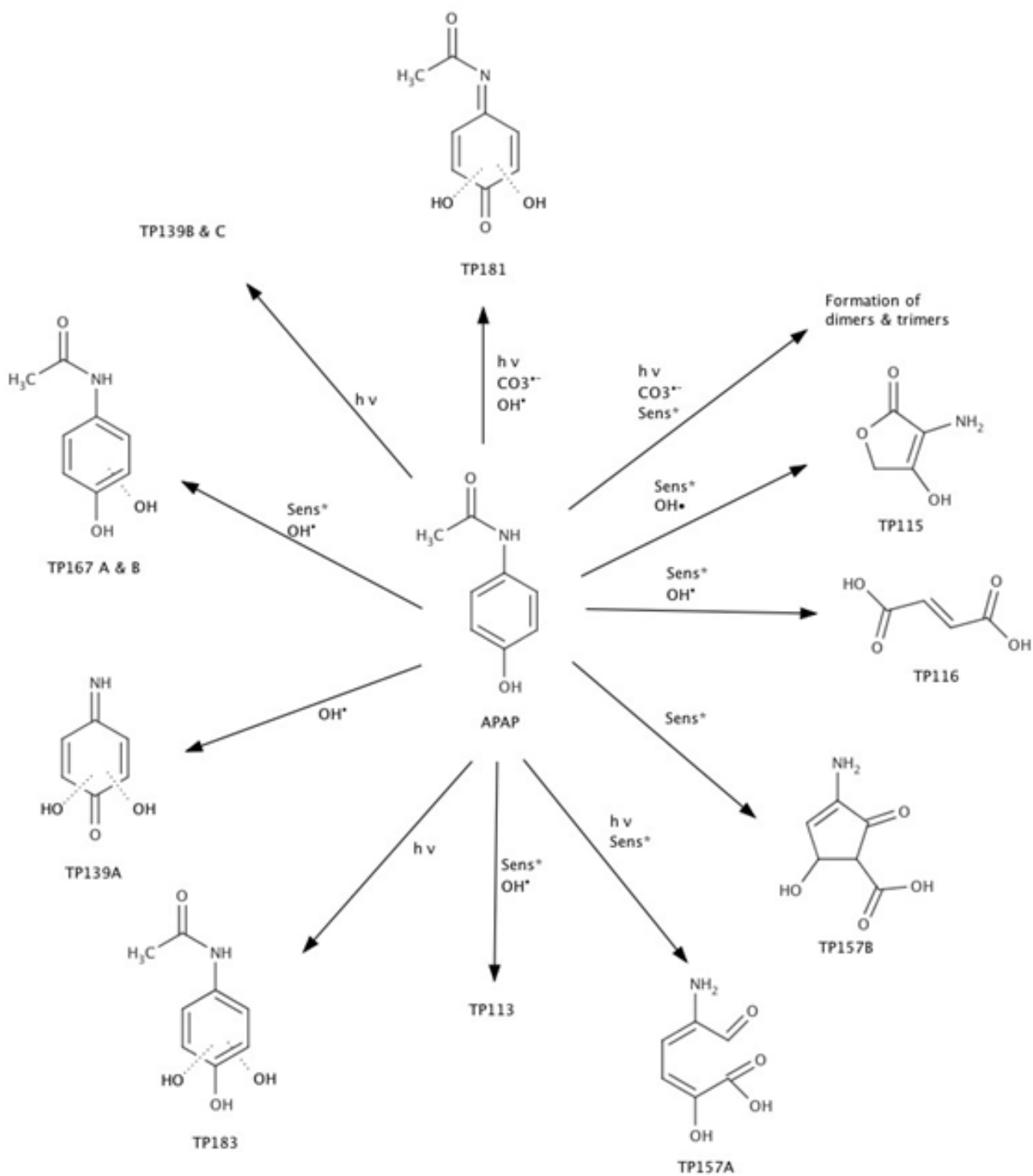
Figure 3. Formation of TPs from 1 mM APAP by direct (hv) and indirect photochemistry, with 1 mM AQ2S (Sens*), 10 mM H_2O_2 ($^\bullet$OH) and 0.1 M $NaNO_3$ + 1 M $NaHCO_3$ ($CO_3^{-\bullet}$, pH 8.5).
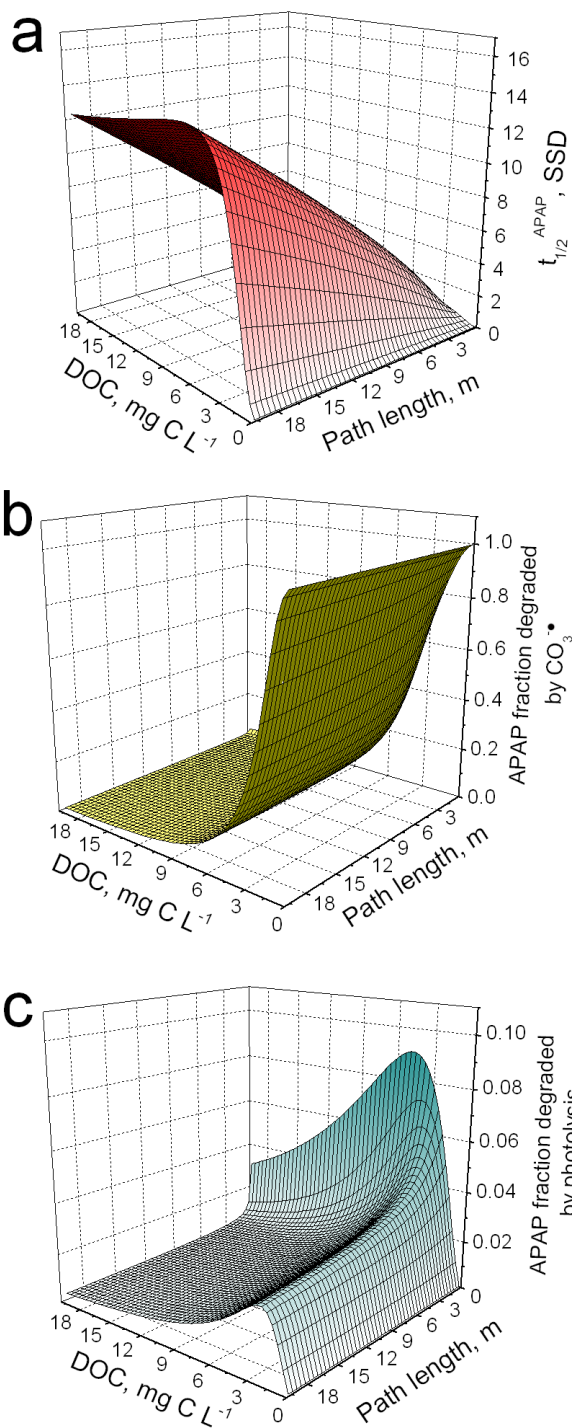
Figure 4. (a) Modelled APAP half-life time, as a function of DOC and of sunlight optical path length. Other water conditions: 0.1 mM NO_3^-, 1 μM NO_2^-, 1 mM HCO_3^-, 10 μM CO_3^{2-} (pH ~ 8). SSD means summer sunny day, equivalent to 15 July at 45°N latitude.
(b) Modelled fraction of APAP that is degraded by $CO_3^{-\bullet}$, as a function of DOC and sunlight path length. Other water conditions as above.
(c) Modelled fraction of APAP that is degraded by direct photolysis, as a function of DOC and sunlight path length. Other water conditions as above.
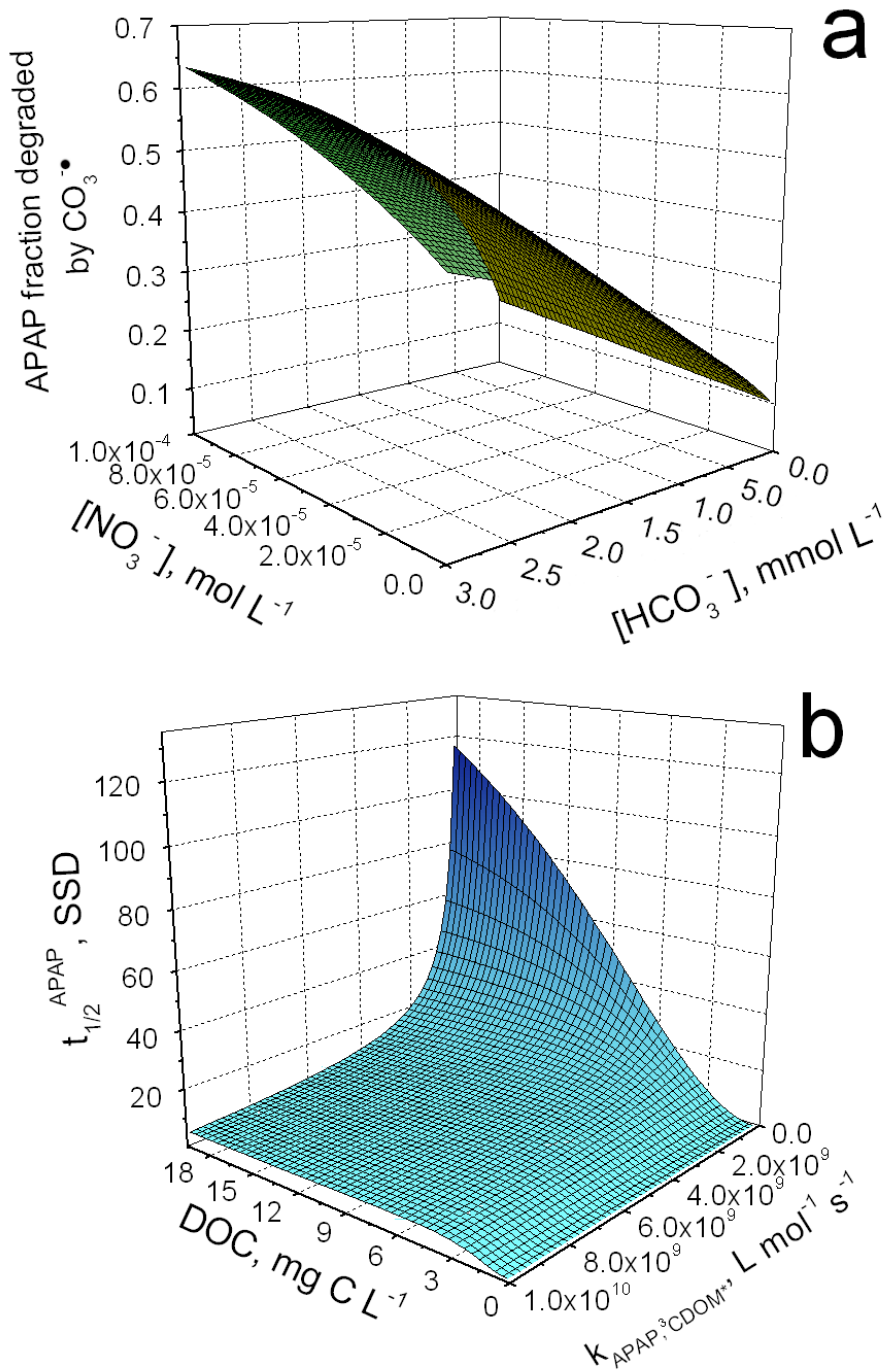
Figure 5. **(a)** Modelled fraction of APAP that is degraded by $CO_3^{-\bullet}$, as a function of NO_3^- and HCO_3^-. Other water conditions: 5 m path length, 3 mg C L^{-1} DOC, 1 μM NO_2^-, 10 μM CO_3^{2-}.

(b) Modelled half-life time of APAP, as a function of DOC and $k_{APAP,^3CDOM*}$. Other conditions: 5 m path length, 0.1 mM NO_3^-, 1 μM NO_2^-, 1 mM HCO_3^-, 10 μM CO_3^{2-} (pH ~ 8).